Occurrence and core-envelope structure of 1–4× Earth-size planets around Sun-like stars

Geoffrey W. Marcy[a,1], Lauren M. Weiss[a], Erik A. Petigura[a], Howard Isaacson[a], Andrew W. Howard[b], and Lars A. Buchhave[c]

[a]Department of Astronomy, University of California, Berkeley, CA 94720; [b]Institute for Astronomy, University of Hawaii at Manoa, Honolulu, HI 96822; and [c]Harvard-Smithsonian Center for Astrophysics, Harvard University, Cambridge, MA 02138

Small planets, 1–4× the size of Earth, are extremely common around Sun-like stars, and surprisingly so, as they are missing in our solar system. Recent detections have yielded enough information about this class of exoplanets to begin characterizing their occurrence rates, orbits, masses, densities, and internal structures. The *Kepler* mission finds the smallest planets to be most common, as 26% of Sun-like stars have small, 1–2 $R_\oplus$ planets with orbital periods under 100 d, and 11% have 1–2 $R_\oplus$ planets that receive 1–4× the incident stellar flux that warms our Earth. These Earth-size planets are sprinkled uniformly with orbital distance (logarithmically) out to 0.4 the Earth–Sun distance, and probably beyond. Mass measurements for 33 transiting planets of 1–4 $R_\oplus$ show that the smallest of them, $R < 1.5\ R_\oplus$, have the density expected for rocky planets. Their densities increase with increasing radius, likely caused by gravitational compression. Including solar system planets yields a relation: $\rho = 2.32 + 3.19 R/R_\oplus$ [g cm^{-3}]. Larger planets, in the radius range 1.5–4.0 $R_\oplus$, have *densities* that decline with increasing radius, revealing increasing amounts of low-density material (H and He or ices) in an envelope surrounding a rocky core, befitting the appellation "mini-Neptunes." The gas giant planets occur preferentially around stars that are rich in heavy elements, while rocky planets occur around stars having a range of heavy element abundances. Defining habitable zones remains difficult, without benefit of either detections of life elsewhere or an understanding of life's biochemical origins.

extrasolar planets | astrobiology | SETI

NASA's *Kepler* mission astonishingly revealed a preponderance of planets having sizes between 1 and 4 times the diameter of Earth (1–5). Our solar system has no planets larger than Earth and smaller than Neptune (3.9 $R_\oplus$). As such, these new planets are poorly understood. Uranus and Neptune provide clues: they have rocky cores of ~10 $M_\oplus$, enveloped by modest amounts of H and He gas. However, the clues are limited by the difficulty in explaining only modest amounts of gas with standard models of runaway gas accretion in the protoplanetary disk (6–9). Planet formation models face another challenge, as they predicted very few planets with final sizes 1–4 $R_\oplus$ (10–12).

This great population of sub-Neptune-mass exoplanets had first been revealed by precise Doppler surveys of stars within 50 parsecs (pc) (13, 14), a finding that *Kepler*'s discoveries confirm. While most of the over 3,000 1–4 $R_\oplus$ planets found by *Kepler* are officially only "candidates," 90% of those candidates are real planets (5, 15, 16). After accounting for detection efficiencies, one may calculate the occurrence rate of small planets, which reveals that the majority of planets orbiting within 1 AU (the distance from Sun to Earth) of solar-type stars, both those near (RV surveys; i.e., radial velocity surveys that measure the wobble of the star by the Doppler effect) and far (*Kepler* survey), are smaller than Uranus and Neptune (i.e., < ~4 $R_\oplus$), as described below.

Occurrence Rates of 1–4 R⊕ Planets

Kepler is superior to RV surveys for measuring occurrence rates of planets down to 1 $R_\oplus$ because it is better at detecting those planets. The Doppler reflex velocity of an Earth-size planet orbiting at 0.3 AU is only 0.2 m s^{-1}, difficult to detect with an observational precision of 1 m s^{-1}. However, such Earth-size planets show up as a ~10-sigma dimming of the host star after coadding the brightness measurements from each transit.

The occurrence rate of Earth-size planets is a major goal of exoplanet science. With three years of *Kepler* photometry in hand, two groups worked to account for the detection biases in *Kepler* planet detection caused by photometric noise, orbital inclination, and the completeness of the *Kepler* transiting-planet detection pipeline (4, 5, 17). They found that within 0.25 AU of solar-type stars, small planets of 1–3× the size of Earth orbit ~30 ± 5% of Sun-like stars. In contrast, only 2 ± 1% have larger planets of Neptune size (4–6 $R_\oplus$), and only 0.5% have Jupiter-size planets (8–11 $R_\oplus$) orbiting that close (4, 17). Intriguingly, the occurrence rate of close-in Jupiter-size planets found around stars in the *Kepler* field of view seems to be about half that found around nearby stars, a difference not understood (18).

A new planet search of nearly 4 y of *Kepler* photometry revealed planets as small as 1 $R_\oplus$ and orbital periods up to 200 d (19). In this tour de force, found 603 planets were found, including 8 planets having sizes 1–2 $R_\oplus$ that receive 1–4× the incident stellar light flux that the Earth enjoys. This new search accounted for detectability efficiency of the smallest, Earth-size planets by injecting into the *Kepler* brightness measurements synthetic dimmings caused by fake planets, and noting the detection success rate. This "injection and recovery" of fake Earth-size planets yields a quantitative correction for efficiency, allowing determination of the true occurrence rate of Earth-size planets.

Fig. 1 shows the resulting fraction of Sun-like stars having planets of different sizes (19) with orbital periods of 5–100 d. The

Significance

Among the nearly 4,000 planets known around other stars, the most common are 1–4× the size of Earth. A quarter of Sun-like stars have such planets orbiting within half an Earth's orbital distance of them, and more surely orbit farther out. Measurements of density show that the smallest planets are mostly rocky while the bigger ones have rocky cores fluffed out with hydrogen and helium gas, and likely water, befitting the term "mini-Neptunes." The division between these two regimes is near 1.5 $R_\oplus$. Considering exoplanet hospitality, 11% of Sun-like stars have a planet of 1–2× the size of Earth that receives between 1.0–4.0× the incident stellar light that our Earth enjoys. However, we remain ignorant of the origins of, and existence of, exobiology, leaving the location of the habitable zone uncertain.
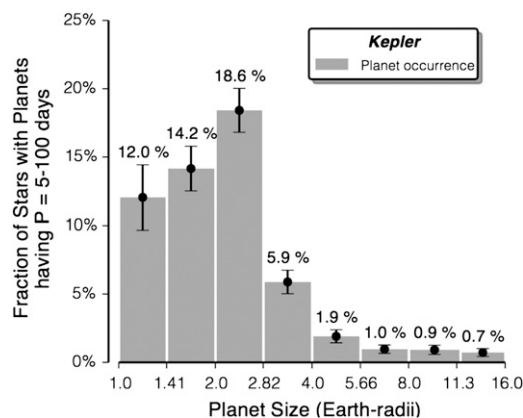
Fig. 1. The size distribution for planets around Sun-like stars. The fraction of Sun-like stars (G- and K-type) hosting planets of a given planet radius are tallied in equal logarithmic bins. Only planets with orbital periods of 5–100 d (corresponding to orbital distances of 0.05–0.42 AU) are included. Together, the lowest two bins show that 26% of Sun-like stars have planets of 1–2 $R_\oplus$ orbiting within ~0.4 AU. The occurrences of Neptune-size planets (2.8–4 $R_\oplus$) and gas-giant planets (8–11 $R_\oplus$) are 5.9% and 0.9%, respectively, more rare than Earth-size planets (19).

lowest two bins show that 26.2% of Sun-like stars have a planets of size, 1–2 $R_\oplus$, with orbital periods under 100 d. Planets as large as Jupiter (11.2 $R_\oplus$) and Saturn (9.5 $R_\oplus$) are more rare, occurring around less than ~1% of Sun-like stars in such orbits. We do not know if the drop-off for the smallest planets is real, a statistical fluctuation, or an incomplete bias correction.

Fig. 2 shows the resulting occurrence rate of planets around Sun-like stars as a function of orbital period. The rate is about 15% at all orbital periods, within bins of multiples of orbital period (i.e., 10–20 d, 20–40 d, 40–80 d), as shown in Fig. 2. This constant planet occurrence with increasing orbital distance, in equal logarithmic bins, surely informs planet formation theory. Indeed, we know of no theoretical cause of major discontinuities in planet formation efficiency inside 1 AU. No phase changes of major planet-building material occur in that region. A smoothly varying occurrence rate, both observed and theoretically, supports mild extrapolations of planet occurrence rates beyond orbital periods of 100 d where the measured rates are empirically secure (19).

Spectroscopy of the host stars of the Earth-size planets yields their luminosities, providing a measure of the incident stellar light fluxes falling on the planets. This analysis shows 11% of Sun-like stars have a planet of 1–2 $R_\oplus$ that receives 1–4× the incident stellar flux that warms our Earth. We note that all 10 such planets detected in Petigura et al. (19) orbit stars with sizes 0.5–0.8 solar radii, i.e., smaller than the Sun. The occurrence of Earth-size planet for Sun-size stars may be somewhat different. It is likely that a similar number of Sun-like stars (11%) have 1–2 $R_\oplus$ planets that receive 1/4–1× the incident flux that Earth enjoys. Thus, if one were to extrapolate to planets receiving 1/4–1× the incident flux of Earth, ~22% of Sun-like stars have a 1–2 $R_\oplus$ planet that receives warming starlight within a factor of 4 of that enjoyed by our Earth, yielding similar surface temperatures, depending on surface reflectivity and greenhouse effects.

Properties: Masses, Radii, and Densities

Although 1–4 $R_\oplus$ planets are common, the theory of their interior structures and chemical compositions is under active investigation (20–28). The measured radii, masses, and densities of small planets constrain the relative amounts of iron and nickel, silicate rock, water, and H and He gas inside the planets. However, the measurements of planet radius and mass leave

degeneracies in the interior composition. Even Uranus and Neptune, which have precisely measured gravitational fields, have compositional degeneracies (29). The interior compositions of small exoplanets are similarly compromised by the possible different admixtures of the rock, water, and gas. Nonetheless, systematic correlations surely exist between planet mass, radius, orbital distance, and stellar type (28, 30–32), making measurements of exoplanet radii and masses useful for understanding the key processes of their formation.

Radii of exoplanets are measured based on the fractional dimming of host stars as planets transit and are known for all *Kepler* objects of interest. Planet masses require additional observations, and stem from Doppler-measured reflex motion of the host star or from variations in the cadence of the planet crossing in front of the star each orbit (transit-timing variations, TTV) caused by planets pulling gravitationally on each other.

To date, 33 planets of 1–4 $R_\oplus$ have measured radii and masses with better than 2-σ quoted accuracy. The *Kepler* Team recently announced the masses and radii of 16 small transiting planets, doubling the number of such well-studied planets (16), and the TTV of Kepler-11 planet system and other Kepler Objects of Interest (KOI) have provided additional measured masses (32–34).

Fig. 3 shows two representative applications of the Doppler technique to determine planet masses for Kepler-78 and Kepler-406. Each star reveals repeated dimmings in *Kepler* photometry due to their transiting planets with orbital periods of 8.5 h and 2.43 d (2), giving planet radii of 1.20 and 1.41 $R_\oplus$, respectively. Doppler measurements exhibit periodicites in phase with the orbit, yielding the reflex velocities of the star and hence the masses of both planets, 1.69 and 4.71 $M_\oplus$, respectively. The resulting densities of the two planets are 5.3 ±1.8 g cm^{-3} and 9.2 $\pm$ 3.3 g cm^{-3}, respectively, both consistent with a purely rocky interior (16, 35, 36). (For reference, the Earth's bulk density is 5.5 g cm^{-3}.) These Doppler measurements are expensive, requiring ~45-min exposures with the world's largest telescopes on 50–100 different nights, while maintaining a Doppler zero-point with a precision of 1 m s^{-1}, i.e., measuring wavelengths to nine significant digits.

In the analysis that follows, we include both Doppler-determined and TTV-determined planet masses. It is worth noting that the TTV planet masses are mostly lower than the RV-determined masses for given radii (although Doppler and TTV measurements of the same planets agree), for reasons not understood (32). Perhaps multiplanet systems, which allow TTV
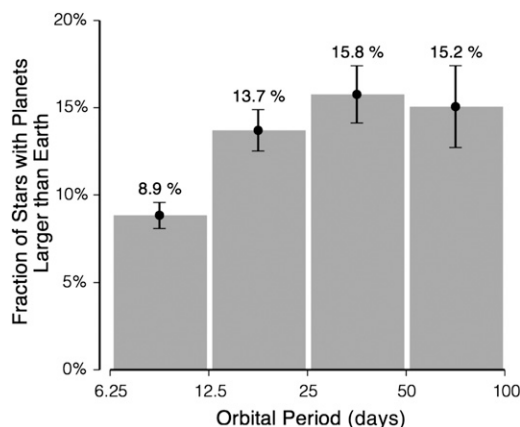

Fig. 2. The fraction of Sun-like stars having planets larger than Earth and within ~0.4 AU, as a function of the planets' orbital periods (log scale). The occurrence of planets is roughly constant, ~15%, in period bins sized by equal factors of 2 in orbital period between 12 and 100 d. Thus, planet occurrence is roughly constant with orbital distance, dN/dlog a = constant, in the inner regions of planetary systems (19).
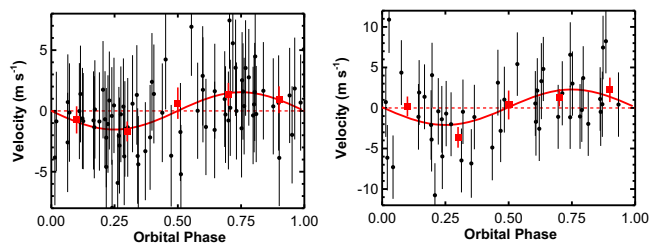
Fig. 3. Doppler measurements made during the orbits of the exoplanets Kepler-78 (*Left*) and Kepler-406 (*Right*), stars that harbor planets with radii of 1.20 and 1.41 $R_\oplus$, respectively. The Doppler measurements show a sinusoidal periodicity, yielding masses corresponding to densities of 5.3 ± 1.8 g cm^{-3} and 9.2 ± 3.3 g cm^{-3}, implying rocky compositions (16, 36).

measurements, survive dynamically only if the planet masses are low enough to limit catastrophic dynamical chaos.

All 33 transiting 1–4 $R_\oplus$ planets with measured radii, (>2-σ) masses, and densities were vetted in detail (32). We explore the interdependencies among these three measured quantities for 1–4 $R_\oplus$ planets in Figs. 4 and 5. Fig. 4 shows planet density as a function of radius for all 33 known exoplanets smaller than $4\,R_\oplus$ (dots). We also include Mars, Venus, and Earth (diamonds at left) and Uranus and Neptune (diamonds at right) as touchstones. The planets reveal a dichotomy in their densities: those larger than 2 $R_\oplus$ are, with one exception, lower density than Earth, indicating their interiors contain substantial volumes of nonrocky, low-density material. For planets larger than 1.5 $R_\oplus$, density declines with increasing radius; bigger planets have increasing amounts of low-density gas.

By contrast, the smallest planets (1–1.5 $R_\oplus$) all have measured densities above 5 g cm^{-3}, consistent with interiors of rock (silicate) and iron–nickel. Indeed, although the scatter is large, the planets smaller than 1.5 $R_\oplus$ have measured densities that increase with increasing radius (left side of Fig. 4). The highest densities occur near a planet radius of ~1.5 $R_\oplus$, at which value the average planet density is 7.6 g cm^{-3} (32, 37), indicating purely rocky interiors.

Among the prominent examples of planets with size 1.5–4.0 $R_\oplus$ and subrocky densities are GJ 1214 b (38–41) with a radius of 2.68 $R_\oplus$ and a mass of only 6.55 $M_\oplus$, yielding a bulk density of 1.87 g cm^{-3}. For comparison, Uranus and Neptune have densities of 1.27 and 1.63 g cm^{-3}, respectively, well below Earth's (5.51 g cm^{-3}). Similarly, the five inner planets around Kepler-11, as well as the exoplanets GJ 3470 b, 55 Cnc e, and Kepler-68 b, all have densities less than 5 g cm^{-3}, with some under 1 g cm^{-3} (33, 42–46). Thus, as shown in Fig. 4, planets of 2–4 $R_\oplus$ have densities too low to be mostly rock by volume.

Even larger planets, 4–6 $R_\oplus$, have densities that are even lower, near 1.0 g cm^{-3} (47, 48). Jupiter and Saturn in our solar system similarly have densities near unity, due to large amounts of gas. Similarly, the sub-Earth bulk densities of planets larger than 2 $R_\oplus$ indicate that they contain significant amounts of H and He and probably some water (49–52).

In contrast, the following planets with radii less than 2 $R_\oplus$ all have 2-σ measured densities over 5 g cm^{-3}: CoRoT 7b, Kepler-10b, Kepler-36b, KOI-1843.03, Kepler-78b, Kepler 406b, Kepler 100b, Kepler 113b, and Kepler 99b (16, 35, 36, 53–57). These are the known rocky exoplanets, all validated as real at the 99% confidence level. All of them are smaller than 1.5 $R_\oplus$.

Thus, we find a density dichotomy, with the dividing radius being near 1.5 $R_\oplus$. Planets smaller than 1.5 $R_\oplus$ have densities consistent with a predominantly rocky interior, while those larger than 1.5 $R_\oplus$ appear to contain increasing amounts of gas with increasing radius (28, 30, 31, 37, 52).

Structure: Core-Envelope Model of 1–4 $R_\oplus$ Planets

The two domains of 1–4 $R_\oplus$ planets, separated at 1.5 $R_\oplus$, motivate separate treatment of the mass–radius relationship in each domain. An empirical fit to the density–radius relation provides a way to explore the ratio of rocky to low-density material in some detail. We fit a linear relation to density as function of radius for all planets smaller than 1.5 $R_\oplus$. We restrict ourselves to a linear relation in this domain because the density measurements have large errors and because of the modest compressibility of rock.

In performing the weighted fit, we include all 22 exoplanets with radius and mass measurements, regardless of the quality of the mass measurement, to mitigate any bias in mass (32). This linear fit includes the four solar system rocky planets with uncertainties of 10% in density so that they do not dominate the fit. We note that both the exoplanets and solar system planets exhibit an increase in density with increasing radius. The mass–density dependence for exoplanets is anchored with Kepler-78b having $R = 1.2\,R_\oplus$ and ρ=5.3–5.6 g cm^{-3} while the other exoplanets between 1.4–1.5 $R_\oplus$ have mostly higher densities between 7 and 14 g cm^{-3}, albeit with large uncertainties (Fig. 4).

By including exoplanets having measured masses that are marginally significant, we promote a statistically useful representation of planets of all masses at a given planet radius (16, 32, 37). For all planets smaller than 1.5 $R_\oplus$, a linear fit to density as a function of radius yields

$$\rho = 2.32 + 3.19 R/R_\oplus \quad (\text{for } R < 1.5 R_\oplus)$$

as described in (32). This linear relation is displayed as the dashed line in Fig. 4, and is translated into a mass–radius relation in Fig. 5. The linear relation reveals a modest increase in density with increasing planet size up to 1.5 $R_\oplus$, likely due to gravitational compression. Among the exoplanets alone (without the solar system planets), the apparent rise in density with radius hinges precariously on the smallest exoplanet, Kepler-78b. We emphasize that the two constants in this linear relation are heavily
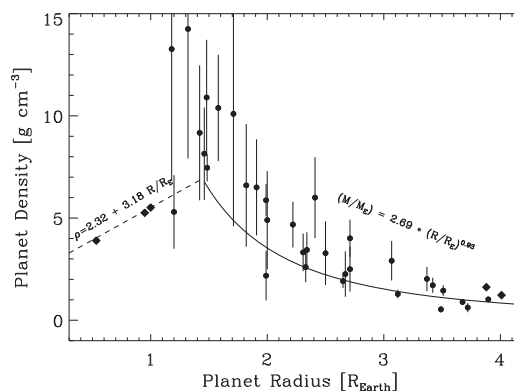

Fig. 4. Planet density vs. radius for all 33 known exoplanets smaller than 4 $R_\oplus$ that have 2-σ mass determinations. Venus, Earth, Mars, Uranus, and Neptune are included (diamonds). The radius of ~1.5 $R_\oplus$ has the highest densities, and marks the transition between rocky planets (smaller size, at left) and planets with increasing amounts of low density material (larger size, at right) (28, 32, 37). For radii 0–1.5 $R_\oplus$, density increases with planet radius, consistent with a purely rocky constitution. In the radius range of 1.5–4.0 $R_\oplus$, density decreases with radius, indicating increasing amounts of H and He gas or water. The transition radius at 1.5 $R_\oplus$ has a density maximum near ~7.6 g cm^{-3} (weighted average). A linear fit including all planets (including sub-2-σ densities, not shown) for $R < 1.5\,R_\oplus$ (dashed line) yields: $\rho(R) = 2.32 + 3.19 R/R_\oplus$ in units of g cm^{-3}. A fit for $R > 1.5\,R_\oplus$ (solid line) yields a density law: $\rho(R) = 2.69 (R/R_\oplus)^{0.93}$ in g cm^{-3}, consistent with a characteristic core mass of roughly 10 $M_\oplus$ (28, 32).
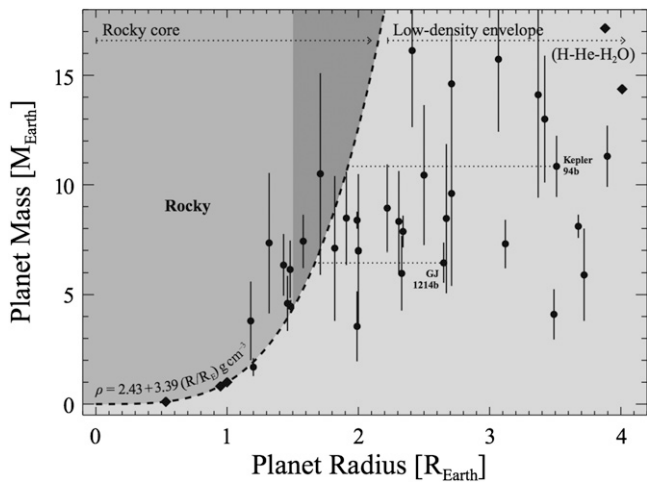
Fig. 5. Planet mass vs. radius, including both the 33 known exoplanets smaller than 4 $R_\oplus$ with 2-σ mass determinations (circles) and the solar system planets (diamonds). Planet mass is correlated with radius in the domain $R < 1.5$ $R_\oplus$. The dashed line marked "rocky" represents the linear density–radius relation from Fig. 4, projected into mass–radius space. The points residing near that dashed line represent planets that must be mostly rocky. The points residing to the right of the "rocky" dashed line represent planets with radii too large to be purely rocky. For such planets, the dashed line represents a simple approximation of the dividing line between a rocky core and a low-density envelope: The horizontal distance to the left of the dashed line (dark gray) represents the radius of the rocky core, while the horizontal distance to the left of the dashed line (light gray) represents the extra radius from the low-density material (H and He or water) in the envelope, which contributes extra size but negligible mass; see refs. 28, 30, 32, 37, 61, 62, and 65. As an example, the additional size, on top of the rocky core, contributed by the H and He or H_2O envelopes for GJ 1214b and for Kepler-94b are indicated by dotted lines. Planets of 1–4 $R_\oplus$ are well modeled by a rocky core containing most of the mass plus a low-density envelope, if any, that enlarges the planet's radius.

influenced by the terrestrial planets in our solar system that reside at larger orbital distances. This linear relation thus stems from a mélange of small planets orbiting both close in and farther out.

For all planets larger than 1.5 $R_\oplus$, a power-law fit to mass as a function of radius is adequate to accommodate the apparent curvature in the mass–radius measurements. The resulting power-law fit yields

$$M/M_\oplus = 2.69(R/R_\oplus)^{0.93} \quad (\text{for } R > 1.5R_\oplus)$$

as described in (32). This mass–radius relation for 1.5–4.0 $R_\oplus$ planets is shown as the solid line in the right half of Fig. 4. Planet density apparently declines with radius, indicating increasing amounts of low-density material as planet radius increases. The solid curve in the right half of Fig. 4 ($R > 1.5R_\oplus$) resides systematically below the plotted points because the curve represents a power-law fit to all known exoplanets in that domain, while we have elected to plot only those points having mass measurements better than 2 σ for visual clarity.

Fig. 5 shows measured planet mass vs. radius for all 33 planets having a mass measurement better than 2 σ. As in Fig. 4, the dashed line shows the previously described linear fit to density vs. radius for all planets smaller than 1.5 $R_\oplus$, likely composed of mostly rocky material. We consider the existence of an envelope of low-density material on top of a rocky core by extending the dashed line to radii greater than 1.5 $R_\oplus$.

With such a linear extrapolation of the density relation, we can make an approximate prediction of the interior structure of planets larger than 1.5 $R_\oplus$. At a given mass, the dashed line represents an estimate of the size of the planet's rocky core. The size of a planet's low-density envelope, therefore, is represented

by the horizontal distance between the dashed line and the plotted point for that planet. Consider the two examples of GJ 1214b and Kepler-94b, with dotted lines drawn from the planet's location in mass–radius space back to the radius representing their rocky cores (dashed line). The lengths of the dotted lines represent the additional radius, on top of any rocky core, that must consist of low-density material to explain the enlarged radius at a given mass.

Thus, cloud of planets residing to the right of the "rocky" dashed line in Fig. 5 support a model of exoplanet structure with both rock and volatiles. These planets have larger radii (and volumes) than can be explained by a purely rocky interior. Therefore, these planets surely contain large amounts of gas and ices to account for their large size, given their mass. Clearly, the planets larger than 2 $R_\oplus$ are composed of large contributions of gas in addition to any rocky core.

A core-envelope model follows from the expectation that the more dense material will sink (differentiate) toward the center of the planet. The argument presented here for large amounts of low-density material on a rocky core does not make use of any theoretical equation of state. The low-density material, presumably H and He gas, must exist in the planets larger than 2 $R_\oplus$ on observational grounds alone.

Interiors, Formation, and Evolution

The range of sizes of rocky planets is visible in Figs. 4 and 5 as the observed rise in density and mass with increasing radius for planets smaller than 1.5 $R_\oplus$. It is an extraordinary accomplishment in planetary astrophysics that the accurately determined radii, masses, and densities of planets smaller than 1.5 $R_\oplus$ reveal increasing mass with radius, signaling their rocky interiors and associated gravitational compression. A linchpin is Kepler-78b that has radius 1.2 $R_\oplus$ and density 5.3 g cm^{-3}, compared with the handful of exoplanets of radius 1.4–1.5 $R_\oplus$ that all have higher densities, displaying gravitational compression and supporting the linear relation for $\rho(R)$ in Figs. 4 and 5. Of course, Mars, Venus, and Earth also exhibit increasing density with radius, offering further support.

For those planets larger than 1.5 $R_\oplus$, the dramatically decreasing density with increasing radius, visible in Fig. 4, clearly indicates increasing amounts of volatiles. Extrapolating the mass–radius relation for purely rocky planets gives an approximate division of the core and envelope for these "mini-Neptunes." The dotted lines in Fig. 5 give an example of this division. However, that division is certainly too simple: Planets of a given radius must also have a diversity of rocky core masses and radii (28, 32). Because most of the mass resides in the core, not the gaseous envelope, only a diversity of rocky core sizes can explain, at a given radius, the observed spread of planets' masses. Thus, the cloud of points in the right halves of Figs. 4 and 5 represent planets with a range of both core masses and volatile content.

The existence of two planet domains on either side of 1.5 $R_\oplus$ is consistent with planet formation models that suppose an accumulation of rocky material up to some critical rocky core mass, followed by accretion of H and He gas. The sequence of planets from 1 to 4 $R_\oplus$ is then interpreted as a sequence of various amounts of iron–nickel and rocky material with either no or increasing amounts of accreted gas (11, 52, 58–64).

The spread in planet bulk densities at a given radius or mass may also be due to the subsequent photoevaporation of volatiles. Such evaporation may be germane because nearly all of the 1–4 $R_\oplus$ planets described here orbit within 0.1 AU of a host FGKM-type star, and therefore their envelopes would be subject to heating, UV deposition, and atmospheric escape (52, 61, 62, 65). These mechanisms for loss of envelopes, along with models of in situ formation of mini-Neptunes, seem to predict the range of sizes, masses, and densities that are observed for the 1–4 $R_\oplus$ planets (28). Detailed models of planet interiors, including the range of chemical compositions, stratified differentiation, and
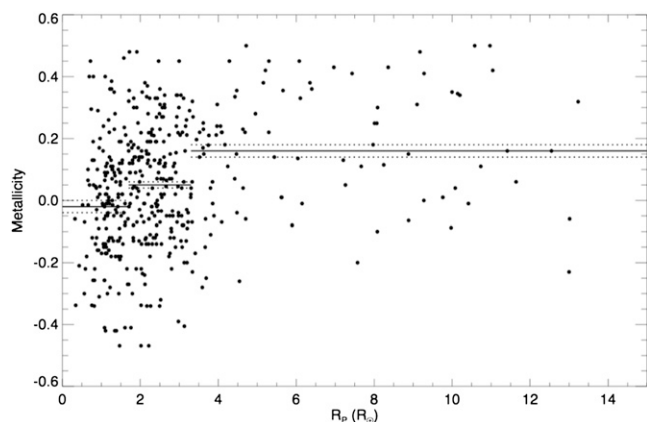
Fig. 6. Abundance of heavy elements (metallicity) of the host star vs. planet radius for over 400 stars as a function of the size of the *Kepler* planet orbiting it. The planets with sizes larger than 4 $R_\oplus$ have host stars relatively rich in heavy elements. In contrast, the smaller planets orbit stars that are roughly solar-like in metallicity. The explanation may be that high metallicity in the proplanetary disk allowed rocky cores to form quickly, before the gas in the disk vanished, allowing the cores to gravitationally accrete that gas to make gas-rich planets.

equations of state, are needed to predict the plausible bulk densities associated with planets with a given mass (8, 23, 24, 28, 37).

Correlations with Heavy Element Abundance

The abundances of heavy elements in the protoplanetary disks around young stars may influence the efficiency of formation of the rocky cores made of such elements. Spectra of the brightest *Kepler* host stars of transiting planets were analyzed by Buchhave et al. (66) to yield their abundances of heavy elements relative to the Sun ("metallicities"). The planets with sizes greater than 3.5 $R_\oplus$ orbit host stars that have, on average, high metallicity: They are rich in heavy elements relative to the Sun. Fig. 6 shows the metallicity on a log scale (zero being solar) of over 400 stars that host ~600 *Kepler* exoplanets (66). Fig. 6 shows that planetary systems seem to fall into three populations defined by different radii and associated stellar metallicities. The smallest planets ($R < 1.7\ R_\oplus$) have, on average, host stars with metallicities slightly less than that of the Sun. The largest planets ($R > 3.4\ R_\oplus$) orbit stars having systematically higher metallicities than the Sun.

One possible explanation for this correlation between planet size and the metallicity of the host star is that giant planets are created from a rocky core that accretes H and He gas from the protoplanetary disk. However, the gas in protoplanetary disks dissipates quickly (within a few million years). The heavy elements in the protoplanetary disk must form a rocky core quickly enough to accrete the gas before it vanishes. If so, the core can accrete H and He gas to form the low-density, gaseous planet. Those stars (and their protoplanetary disks) that have only modest metallicity (or less) form rocky cores more slowly, after most of the gas in the protoplanetary disk has vanished, leaving only rocky cores that are devoid of a gaseous envelope (66). If this explanation is roughly correct, the Earth resides at a planetary sweet spot, coming from a protoplanetary disk with inadequate heavy elements to grow quickly enough to grab huge amounts of gas, but adequate to initiate complex biochemistry.

Habitable Zone: Humility and Hubris

Scientific knowledge of complex systems is normally anchored by, and repeatedly tested by, experimental evidence. The planetary conditions necessary for biology certainly qualify as a complex physical, chemical, and biological problem. A common construct toward such discussions is the "habitable zone," the orbital domain around a star where life can arise and flourish. Unfortunately, we have no empirical evidence of life arising, nor of it flourishing, around any other star.

Such lack of experimental evidence of life has not slowed the debate about the exact location of the habitable zone around stars of different types. The passion exhibited in this debate is worthy of some caution. We have no evidence of microbial life at any orbital location within our solar system beside the Earth. We have no empirical information about microbial life as a function of orbital distance from our Sun or from any other star. We also have no evidence of multicellular life around any other star, nor evidence of intelligent life.

Thus, we have no empirical knowledge about the actual domain of habitable zones, for any type of life, around any type of star. Moreover we have virtually no theoretical underpinnings about exobiology. We still do not know how biology started on Earth. We do not know the mechanisms that caused a transition from chemistry to biology, nor do we know the biochemical steps that spawn proteins, RNA, DNA, or cell membranes (67), although there has been recent progress (68). Indeed, we still have a poor definition of life (69).

Our ignorance about both the necessary planetary environments and the complex biochemical pathways for life should urge caution in predicting, with multiple significant digits, the location of the "habitable zones" around other stars. We can't predict if Mars, Europa, or Enceladus have habitable environments any better than we can predict the weather in our hometown a week in advance.

What is needed is a census of biology among a sample of nearby stars, measuring the orbital locations and geological types of planets where biologies exist. A door-to-door census of life among stellar neighbors is needed to answer empirically and with credibility the true domain of habitability around other stars. That census can be carried out three ways: within our solar system among water-bearing planets and moons, by space-borne telescopes that perform chemical assays of resolved rocky planets, and by searches for transmissions from technological beings.

1. Borucki WJ, et al. (2011) Characteristics of planetary candidates observed by Kepler. II. Analysis of the first four months of data. *ApJ* 736(1):19.
2. Batalha NM, et al. (2013) Planetary candidates observed by Kepler. III. Analysis of the first 16 months of data. *ApJS* 204(2):24.
3. Howard AW (2013) Observed properties of extrasolar planets. *Science* 340(6132):572–576.

4. Petigura EA, Marcy GW, Howard AW (2013) A plateau in the planet population below twice the size of Earth. *ApJ* 770(1):69.
5. Fressin F, et al. (2013) The false positive rate of Kepler and the occurrence of planets. *ApJ* 766(2):81.
6. Pollack JB, et al. (1996) Formation of the giant planets by concurrent accretion of solids and gas. *Icarus* 124(1):62–85.

7. Goldreich P, Lithwick Y, Sari R (2004) Planet formation by coagulation: A focus on Uranus and Neptune. *Annu Rev Astron Astrophys* 42:549–601.

8. Rogers LA, Seager S (2010) Three possible origins for the gas layer on GJ 1214b. *ApJ* 716(2):1208–1216.

9. Morbidelli A (2013) *Dynamical Evolution of Planetary Systems*, eds Oswalt TD, French LM, Kalas P (Springer, NY), 63 pp.

10. Ida S, Lin DNC (2010) Toward a deterministic model of planetary formation. VI. Dynamical interaction and coagulation of multiple rocky embryos and super-Earth systems around solar-type stars. *ApJ* 719(1):810–830.

11. Mordasini C, Alibert Y, Klahr H, Henning T (2012) Characterization of exoplanets from their formation. I. Models of combined planet formation and evolution. *Astron Astrophys* 547:A111.

12. Alibert Y, et al. (2013) Theoretical models of planetary system formation: Mass vs. semi-major axis. *Astron Astrophys* 558:A109.

13. Howard AW, et al. (2010) The occurrence and mass distribution of close-in super-Earths, Neptunes, and Jupiters. *Science* 330(6004):653–655.

14. Mayor M, et al. (2011) The HARPS search for southern extra-solar planets XXXIV. Occurrence, mass distribution and orbital properties of super-Earths and Neptune-mass planets. arXiv:1109.2497.

15. Morton TD, Johnson JA (2011) On the low false positive probabilities of Kepler planet candidates. *ApJ* 738(2):170.

16. Marcy GW, et al. (2014) Masses, radii, and orbits of small Kepler planets: The transition from gaseous to rocky planets. *ApJS* 210(2):20.

17. Howard AW, et al. (2012) Planet occurrence within 0.25 AU of solar-type stars from Kepler. *ApJS* 201(2):15.

18. Wright JT, et al. (2012) The frequency of hot Jupiters orbiting nearby solar-type stars. *ApJ* 753(2):160.

19. Petigura EA, Howard AW, Marcy GW (2013) Prevalence of Earth-size planets orbiting Sun-like stars. *Proc Natl Acad Sci USA* 110(48):19273–19278.

20. Seager S, Kuchner M, Hier-Majumder CA, Militzer B (2007) Mass–radius relationships for solid exoplanets. *ApJ* 669(2):1279–1297.

21. Fortney JJ, Marley MS, Barnes JW (2007) Planetary radii across five orders of magnitude in mass and stellar insolation: Application to transits. *ApJ* 659(2):1661–1672.

22. Zeng L, Seager S (2008) A computational tool to interpret the bulk composition of solid exoplanets based on mass and radius measurements. *Pub Astron Soc Pac* 120(871):983–991.

23. Rogers LA, Bodenheimer P, Lissauer JJ, Seager S (2011) Formation and structure of low-density exo-Neptunes. *ApJ* 738(1):59.

24. Zeng L, Sasselov D (2013) A detailed model grid for solid planets from 0.1 through 100 Earth masses. *Pub Astron Soc Pac* 125(925):227–239.

25. Lissauer JJ, et al. (2011) Architecture and dynamics of Kepler's candidate multiple transiting planet systems. *ApJS* 197(1):8.

26. Lissauer JJ, et al. (2012) Almost all of Kepler's multiple-planet candidates are planets. *ApJ* 750(2):112.

27. Fabrycky DC, et al. (2012) Architecture of Kepler's multi-transiting systems: II. New investigations with twice as many candidates. arXiv:1202.6328.

28. Lopez ED, Fortney JJ (2013) Understanding the mass-radius relation for sub-Neptunes: Radius as a proxy for composition. arXiv:1311.0329.

29. Helled R, et al. (2013) Giant planet formation, evolution, and internal structure. arXiv:1311.1142.

30. Fortney JJ, et al. (2013) A framework for characterizing the atmospheres of low-mass low-density transiting planets. *ApJ* 775(1):80.

31. Weiss LM, et al. (2013) The mass of KOI-94d and a relation for planet radius, mass, and incident flux. *ApJ* 768(1):14.

32. Weiss LM, Marcy GW (2014) The mass-radius relation between 63 exoplanets smaller than 4 Earth radii. arXiv:1312.0936.

33. Lissauer JJ, et al. (2013) All six planets known to orbit Kepler-11 have low densities. *ApJ* 770(2):131.

34. Hadden S, Lithwick Y (2013) Densities and eccentricities of 163 Kepler planets from transit time variations. arXiv:1310.7942.

35. Pepe F, et al. (2013) An Earth-sized planet with an Earth-like density. *Nature* 503(7476):377–380.

36. Howard AW, et al. (2013) A rocky composition for an Earth-sized exoplanet. *Nature* 503(7476):381–384.

37. Rogers LA (2014) Glimpsing the compositions of sub-Neptune-size exoplanets. *IAU Symp* 299:247–251.

38. Maness HL, et al. (2007) The M dwarf GJ 436 and its Neptune-mass planet. *Pub Astron Soc Pac* 119(851):90–101.

39. Gillon M, et al. (2007) Detection of transits of the nearby hot Neptune GJ 436 b. *Astron Astrophys* 472(2):L13–L16.

40. Torres G, Winn JN, Holman MJ (2008) Improved parameters for extrasolar transiting planets. *ApJ* 677(2):1324–1342.

41. Charbonneau D, et al. (2009) A super-Earth transiting a nearby low-mass star. *Nature* 462(7275):891–894.

42. Bonfils X, et al. (2012) A hot Uranus transiting the nearby M dwarf GJ 3470. Detected with HARPS velocimetry. Captured in transit with TRAPPIST photometry. *Astron Astrophys* 546:A27.

43. Endl M, et al. (2012) Revisiting ρ^1 Cancri e: A new mass determination of the transiting super-Earth. *ApJ* 759(1):19.

44. Demory B-O, et al. (2013) Spitzer observations of GJ 3470 b: A very low-density Neptune-size planet orbiting a metal-rich M dwarf. *ApJ* 768(2):154.

45. Demory B-O, et al. (2011) Detection of a transit of the super-Earth 55 Cancri e with warm Spitzer. *Astron Astrophys* 533:A114.

46. Gilliland RL, et al. (2013) Kepler-68: Three planets, one with a density between that of Earth and ice giants. *ApJ* 766(1):40.

47. Cochran WD, et al. (2011) Kepler-18b, c, and d: A system of three planets confirmed by transit timing variations, light curve validation, warm-Spitzer photometry, and radial velocity measurements. *ApJS* 197(1):7.

48. Hartman JD, et al. (2011) HAT-P-26b: A low-density Neptune-mass planet transiting a K star. *ApJ* 728(1):138.

49. Figueira P, Pont F, Mordasini C, Alibert Y, Georgy C, Benz W (2009) Bulk composition of the transiting hot Neptune around GJ 436. *Astron Astrophys* 493:671–676.

50. Rogers LA, Seager S (2010) A framework for quantifying the degeneracies of exoplanet interior compositions. *ApJ* 712(2):974–991.

51. Batygin K, Stevenson DJ (2013) Mass-radius relationships for very low mass gaseous planets. *ApJLett* 769(1):L9.

52. Lopez ED, Fortney JJ (2013) The role of core mass in controlling evaporation: The Kepler radius distribution and the Kepler-36 density dichotomy. *ApJ* 776(1):2.

53. Queloz D, et al. (2009) The CoRoT-7 planetary system: Two orbiting super-Earths. *Astron Astrophys* 506:303–319.

54. Batalha NM, et al. (2011) Kepler's first rocky planet: Kepler-10b. *ApJ* 729(1):27.

55. Carter JA, et al. (2012) Kepler-36: A pair of planets with neighboring orbits and dissimilar densities. *Science* 337(6094):556–559.

56. Rappaport S, Sanchis-Ojeda R, Rogers LA, Levine A, Winn JN (2013) The Roche limit for close-orbiting planets: Minimum density, composition constraints, and application to the 4.2 hr planet KOI 1843.03. *ApJLett* 773(1):L15.

57. Sanchis-Ojeda R, et al. (2013) Transits and occultations of an Earth-sized planet in an 8.5 hr orbit. *ApJ* 774(1):54.

58. Chiang E, Laughlin G (2013) The minimum-mass extrasolar nebula: In situ formation of close-in super-Earths. *Mon Not R Astron Soc* 431(4):3444–3455.

59. Hansen BMS, Murray N (2013) Testing in situ assembly with the Kepler planet candidate sample. *ApJ* 775(1):53.

60. Lopez ED, Fortney JJ, Miller N (2012) How thermal evolution and mass-loss sculpt populations of super-Earths and sub-Neptunes: Application to the Kepler-11 system and beyond. *ApJ* 761(1):59.

61. Gillon M, et al. (2012) Improved precision on the radius of the nearby super-Earth 55 Cnc e. *Astron Astrophys* 539:A28.

62. Demory B-O, et al. (2012) Detection of thermal emission from a super-Earth. *ApJLett* 751(2):L28.

63. Lammer H, et al. (2013) The science of exoplanets and their systems. *Astrobiology* 13(9):793–813.

64. Raymond SN, Cossou C (2014) . No universal minimum-mass extrasolar nebula: Evidence against in-situ accretion of systems of hot super-Earths. arXiv:1401.3743.

65. Lammer H, et al. (2013) Probing the blow-off criteria of hydrogen-rich 'super-Earths.' *Mon Not R Astron Soc* 430(2):1247–1256.

66. Buchhave LA, et al. (2012) An abundance of small exoplanets around stars with a wide range of metallicities. *Nature* 486(7403):375–377.

67. Lal A (2008) Origin of life. *Astrophys Space Sci* 317(3-4):267–278.

68. Adamala K, Szostak JW (2013) Nonenzymatic template-directed RNA synthesis inside model protocells. *Science* 342(6162):1098–1100.

69. Szostak JW (2012) Attempts to define life do not help to understand the origin of life. *J Biomol Struct Dyn* 29(4):599–600.